Supplementary Information

Article Ref: B921840H - Soft Matter

Atomistic Simulations of the Wetting Behavior of Nanodroplets of Water on Homogeneous and Phase Separated Self-Assembled Monolayers

J. D. Halverson, C. Maldarelli, A. Couzis and J. Koplik

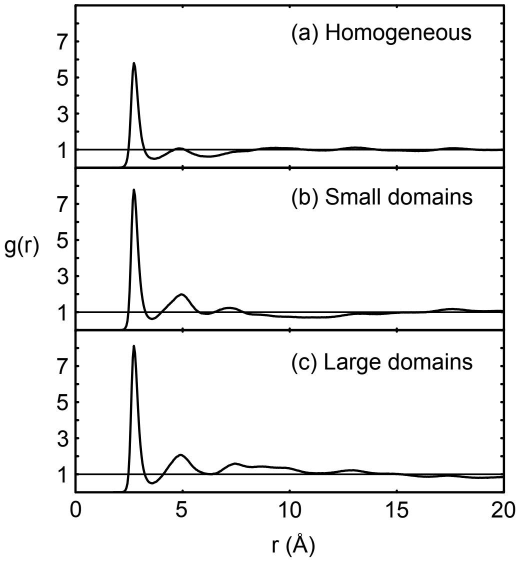

Figure S1: The oxygen-oxygen radial distribution functions for three monolayers with different degrees of phase-separation and $\chi_p = 0.5$. The diameters of the small and large circular domains are 1 and 2 nm.

The oxygen-oxygen radial distribution function (RDF) is shown in Fig. 1 for the homogeneous and phase separated monolayers with $\chi_p = 0.5$. The RDF for the homogeneous monolayer shows a peak of 5.8 at $r = 2.7$ Å. Since the NN separation distance between chains in the monolayer is 4.97 Å this peak comes about by NN chains tilting towards one another to maximize the van der Waals interaction and to form hydrogen bonds. The second peak occurs at $r = 4.8$ Å with a magnitude of 1.1. Little structure is seen in the homogeneous monolayer for separations greater than 7.5 Å. The radial distribution functions for the phase-separated monolayers are shown in Fig. 1b,c. As with the homogeneous case, the phase separated monolayers show a first peak at $r = 2.7$ Å with magnitudes of 7.8 and 8.1 for the 1 nm and 2 nm domains, respectively. The heterogeneous monolayers have similar second peaks, which occur at $r = 4.9$ Å with a magnitude of 2.0. Beyond this distance the behavior of the phase separated monolayers differ. For the case with 1 nm domains the RDF is seen to drop below unity after a small third peak while the RDF for the monolayer with large domains remains above unity until separations of 15.2 Å are reached. The crystallinity of the monolayers gives rise to slight features for large separations.

The procedure of de Ruijter et al. was adopted to determine the equilibrium shape of each droplet. In short, the time-averaged fluid density field is found about the center-of-mass axis of the droplet by assigning molecules to cylindrical bins of volume $\pi\Delta z(r_i^2 - r_{i-1}^2)$, where $r_i = \sqrt{i\Delta A/\pi}$ for $i = 1, 2, ..., n$. Here

χ_p	$\langle z_W \rangle$	$\langle z_D \rangle$	h_0	h_W	h_D
0.00	7.84	7.89	2.19	10.03	10.08
0.25	8.11	8.03	2.07	10.18	10.10
0.50	8.33	8.13	1.96	10.29	10.09
0.75	8.53	8.19	1.84	10.37	10.03
1.00	8.69	8.25	1.72	10.41	9.97

Table S1: The wet and dry heights of the homogeneous monolayers. All values are given in units of Å. h_0 is the sum of the second and third terms in Eqn. 1 (i.e., $h_{W/D} = \langle z_{W/D} \rangle + h_0$).

we use the same parameters as Werder et al. (i.e., $\Delta z = 0.5$ Å and $\Delta A = 95$ Å^2). When the averaging is complete, for each z-slab the smallest value of r_i is determined where the liquid density falls below one half its bulk value. Data points within 5 Å of the top of the monolayer are ignored because the liquid density varies over this region. Similarly, data points a few angstroms from the apex of the droplet are also discarded. The best-fit circle is found for the set of points $\{r_j, z_j\}$ using a nonlinear fitting routine. The contact angle and other properties are determined with knowledge of the height of the monolayer. The best-fit circle, liquid-vapor boundary profile data points, and tangent line at the droplet edge are shown in the main manuscript for the $\chi_p = 0.5$ case.

The height of the monolayer was computed using an approach similar to that of Hautman and Klein. The height is taken as the average z-coordinate of the methyl and oxygen atomic centers, $\langle z \rangle$, plus terms to account for the size of the atoms, h_0:

$$h = \langle z \rangle + (1 - \chi_p)\frac{2^{1/6}\sigma_{\mathrm{CC}}}{2} + \chi_p \frac{2^{1/6}\sigma_{\mathrm{OO}}}{2}, \tag{1}$$

where σ_{CC} is the Lennard-Jones parameter for the CH_3–CH_3 interaction appearing in the force field table. The wet height, h_W, is computed using only chains that are beneath the droplet whereas the dry height, h_D, is based on chains away from the droplet. Table 1 reports the wet and dry heights for each choice of χ_p. The two heights are found to be very similar with the largest difference being 0.44 Å for the $\chi_p = 1$ case. The difference comes about by chains beneath the droplet extending their hydroxyl groups upward to hydrogen bond with water. The dry chains can only hydrogen bond with other chains, which takes place in the plane of the monolayer. All contact angles were calculated using h_W.

The transverse components of the center-of-mass position of each droplet for all time are shown in Fig. 2. The center-of-mass of each droplet begins at the origin and with time it changes due to thermal fluctuations and local gradients in the substrate surface energy. The final position of the droplet is indicated by the open circle in each plot. In general, the displacement from the origin decreases with increasing χ_p for the same time interval. That is, the droplets on

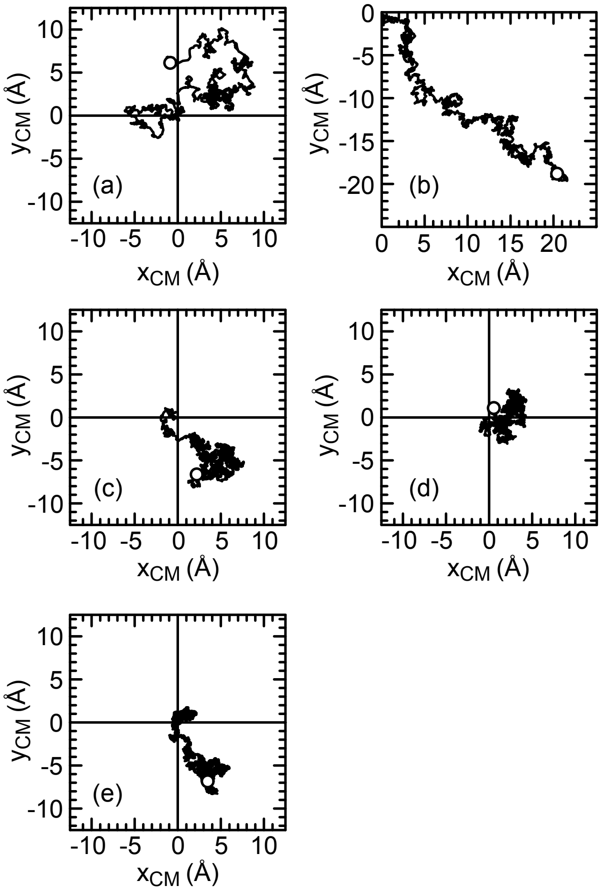

Figure S2: The transverse components of the center-of-mass position of the droplet are shown for all time on a homogeneous monolayer: (a) $\chi_p = 0$, (b) $\chi_p = 0.25$, (c) $\chi_p = 0.5$, (d) $\chi_p = 0.75$, and (e) $\chi_p = 1$. The open circle in each plot indicates the final position of the droplet.

This journal is (c) The Royal Society of Chemistry 2010

the monolayers with $\chi_p = 0$ and 0.25 (Fig. 2a,b) exhibit much more mobility than the $\chi_p = 0.75$ and 1 cases (Fig. 2d,e) which move only a few angstroms.